

LARGE EDDY SIMULATION OF AN AERATED RUSHTON STIRRED REACTOR

D. Arlov^{†,*}, J. Revstedt[†], L. Fuchs[†]

[†]Department of Energy Sciences, Division of Fluid Mechanics, Lund University, Lund, Sweden

*Email: dragana.arlov@vok.lth.se

ABSTRACT

Simulations of aerated stirred reactor is performed using Large Eddy Simulation (LES). The gas phase is modelled using Lagrangian Particle Tracking (LPT). The reactor is stirred by a single impeller Rushton turbine, centred in the reactor. The air is introduced at the bottom wall through a circular sparger. The main focus is to investigate how the gas phase affects the liquid in the reactor. Effects of gas volume flow and stirrer speed are investigated. The results show that the time averaged liquid velocities in the radial and tangential directions as well as the pumping capacity decrease with increasing gas volume fraction. In the axial direction the gas redirects the radial jet upwards breaking the symmetry of the ring vortices.

INTRODUCTION

The dispersion of gases by agitated reactors is used extensively for example in biochemical processes. Issues concerning fluid flow inside the bioreactors are many such as explaining how the trailing vortices behind the impeller blades are affected by aeration and how the mixing in the reactor is influenced by the gas phase. Understanding these features in the reactor is needed to ensure good mixing, essential for keeping a high quality of the product, but also gain knowledge of how to design the reactors optimally. Literature concerning gas-liquid stirred tanks is scarcer as compared to only liquid stirred tanks. Lu and Ju [1] studied the magnitude of liquid flow in a aerated stirred tank using a constant temperature anemometry. They observed that the radial jet is tilted upwards due to the bubble swarm. Using numerical methods, three-dimensional $k - \epsilon$ turbulence models for the liquid phase together with an Eulerian-Eulerian approach for the gas phase, has been used extensively over the years, for ex-

ample Deen [2]. One of the many observations resulted into that the trailing vortices behind the impeller decreases in strength when introducing air bubbles. However, inside a reactor the flow consists of curved streamlines, swirling motion and non-isotropic turbulence, situations where $k - \epsilon$ models are known to produce unreliable results. By using Large Eddy Simulation (LES) these problems can be avoided and additional information is obtained about the time dependent phenomena occurring in the reactor. However, LES requires longer computational time. Wu [7] performed a simulation of a dual-impeller reactor with an Eulerian-Lagrangian approach for the gas-phase.

The purpose of this study is to, by using LES for liquid phase and two-way coupled Lagrangian Particle Tracking (LPT) for gas phase, investigate how the gas phase affects the liquid flow in a reactor at low gas volume fractions. Effects of changing the aeration number and impeller speed are considered.

STIRRED REACTOR CONFIGURATION

The reactor studied in this work is a cylindrical tank with a diameter $T=300$ mm, a height $H=T$, with four equispaced baffles and a Rushton turbine placed at $H/2$, as shown in Figure 1. Furthermore, a circular sparger of diameter $T/4$ is placed at the bottom. Bubbles are introduced through the sparger at two different volume flows, $Q_1 = 2.7 \cdot 10^{-5} \text{ m}^3/\text{s}$ and $Q_2 = 2.7 \cdot 10^{-4} \text{ m}^3/\text{s}$, with 2 bubble diameters (1.5 and 2.0 mm). The gas volume flow was chosen to be low corresponding to a aeration number of $N_A = 0.004$ and $N_A = 0.04$ for Q_1 and Q_2 cases, respectively. The turbine rotates with 400 rpm, corresponding to a Reynolds number of 67000, based on impeller diameter and rotational speed. Additionally, for Q_2 the turbine is also rotated at 300 rpm. The tank is filled with water of density 998 kg/m^3 and the injected air bubbles have a density of 1.2 kg/m^3 .

NUMERICAL METHOD

For the liquid phase, the governing equations are discretised on a Cartesian staggered grid using a third- and fourth-order accurate finite-difference schemes for convective terms and the diffusive terms, respectively. To maintain computational efficiency, the higher order scheme has been embedded into a second order scheme using a single/few step defect correction approach, Gullbrand et al. [4]. A multi-grid method is used to enhance the convergence rate of the implicit solver, within each time step. An implicit SGS model is applied. The truncation error of the numerical scheme is mainly dissipative and acts to dissipate energy at the smallest resolved scales. The major advantage of the implicit model is its simplicity and higher computational speed as compared to an explicit one and it has been used successfully among others, for example by Revstedt et

al. [5] and Gullbrand et al. [4]. For the stationary and rotating solid boundary the Volume of Solid (VOS) method is used, based on the Volume of Fluid (VOF) approach. In VOS, the solid body is assumed to have an infinite viscosity and a averaged viscosity is defined as the fluid viscosity times the inverse of the amount of fluid in each computational cell. Furthermore, cells containing the solid phase will be blocked. The bubbles are expressed using a two-way coupled LPT, where drag, buoyancy, added mass, viscous, pressure and Saffman's lift forces are accounted for. In LPT every bubble is tracked using Newton's second law and each bubble is assumed to be small enough to be treated as a discrete point in a given cell-volume. For the simulations the grid size was chosen to be 2 mm together with a time step of 0.14 ms corresponding to a CFL-number of 0.15. A central issue of using a combination of LES and LPT is the conflicting resolution requirements. LES requires that the grid resolution is of the same order of magnitude as the Taylor micro-scale. However, in order for the effect of the bubble to be considered a local, LPT requires that the volume of the bubble is much smaller than of the computational cell. At the chosen grid resolution the bubbles would occupy 46% and 19% of the volume of a computational cell. This is clearly larger than what is usually considered to be the limit for Lagrangian tracking, and this will of course lower the accuracy of the solution. However, since the volume fractions is very low in most of the tank it is not reasonable to use a Eulerian type model for the dispersed phase. The Stokes number was calculated to 0.014 (for 2 mm bubble) and 0.008 (for 1.5 mm bubble). However, due to the number of bubbles in the tank the momentum coupling term gives the need for two-way coupling LPT when the number of bubbles increases.

RESULTS AND DISCUSSION

The air is introduced at the bottom of the tank and the role of the impeller, apart from accelerating the liquid, is to disperse the bubbles to achieve an even distribution in the bulk of the tank. Fig. 2 shows the gas volume fraction at 400 and 300 rpm in the centre plane of the tank. As can be seen, higher impeller speed increases the dispersion in the upper part of the tank. However, the lower part will for the most part be un-aerated irrespective of the speed. This behaviour has been observed in several previous studies, for example by Friberg and Hjertager [6]. Fig. 3 displays the time averaged liquid velocity in radial, tangential and axial direction. For radial and tangential velocity the single phase simulations are compared to experimental data by Wu and Patterson [7] and LES data by Eggels [8], showing reasonable agreement. In the impeller range, $1.2 < r/R < 2$, the radial and tangential liquid velocity for the aerated case is lower than the un-aerated case and decreases with increasing aeration rate, due to the presence of bubbles. Furthermore, the higher volume flow of gas (Q_2) redirects the flow upwards, which was also observed by Lu and Ju [1] and Deen [2]. The decrease in radial velocity at the impeller discharge is also reflected in the pumping capacity, as can be observed in Fig. 4. The un-aerated tank shows good agreement when compared to existing data and the presence of bubbles decreases the pumping capacity slightly in the range $1.25 < r/R < 1.65$.

The time averaged axial velocity at four axial positions ($z = 2H/8, 3H/8, 5H/8$ and $6H/8$) is shown in Fig. 5. At the lowest position ($2H/8$) one can observe a stronger down flow close to the wall in the aerated cases. This might indicate that the circulation in the lower part of the tank could be promoted by the bubble plume from the sparger. Considering the corresponding position above the impeller, there is a significant change in the axial velocity for the Q_2 -case. Here the

presence of bubbles instead counteracts the circulation.

Fig. 6 depicts the power spectra for the radial velocity fluctuations in the centre of the impeller stream at $r/R = 1.5$. As is expected one observes a peak at the blade passing frequency ($40Hz$) in both the aerated and un-aerated cases. However, the amplitude is lower in the aerated case, which is probably an effect of the bubbles interfering with the trailing vortex pair created behind the blades.

CONCLUSION

Simulations of a tank have been performed with and without gas. From these results it can be concluded that the presence of bubbles decreases the time averaged radial and tangential velocity in the impeller discharge. With increasing aeration rate, the radial jet is redirected upwards creating asymmetric ring vortices and the periodicity from the impellers are less pronounced. Low aeration number gives a marginal influence on the axial velocity as compared to an un-aerated case. Furthermore, inserting gas lowers the pumping capacity in the impeller region. Increasing the rotation rate increases the dispersion of bubbles in the upper part of the tank. However, the lower part of the tank remains almost completely un-aerated.

ACKNOWLEDGEMENT

This work was financed by the Swedish Strategic Research Foundation (SSF). Computational resources were provided by the center for scientific computing at Lund University (LUNARC) and the Swedish National Infrastructure for Computing (SNIC).

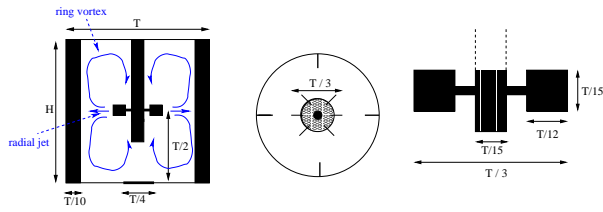


Fig. 1. Cross-section of the reactor, from side (left), from above (middle) and of the impeller (right).

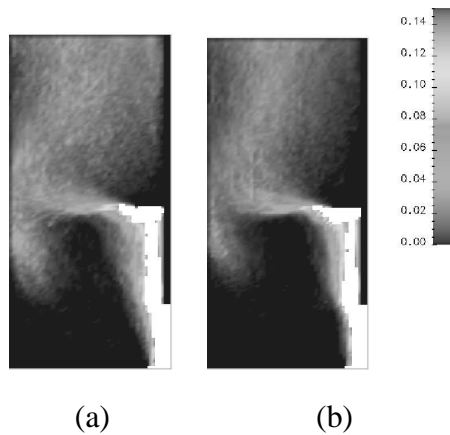


Fig. 2. Time averaged gas fraction in the rz -plane for Q_2 at (a) 400 rpm and (b) 300 rpm. The white areas indicate a gas fraction, $\alpha_g > 0.15$.

BIBLIOGRAPHY

- [1] W.-M. Lu and S.-J. Ju, "Local gas holdup, mean liquid velocity and turbulence in an aerated stirred tank using hot-film anemometry", *Chemical Engineering Journal*, vol. 35, pp. 9-17, 1987.
- [2] N. Deen, "An experimental and computational study of fluid dynamics in gas-liquid chemical reactors," PhD Thesis, Aalborg University Esbjerg, Esbjerg, Denmark, 2001.
- [3] Z. Wu, "Numerical study of dispersed two-phase flows," PhD Thesis, Lund Institute of Technology, Lund, Sweden, 2000.
- [4] J. Gullbrand, X.S. Bai and L. Fuchs, "High order Cartesian grid method for calculation of turbulent flows", *Int. J. Num. Meth. in Fluids*, vol. 36, pp. 687-709, 2001.
- [5] J. Revstedt, J. Gullbrand, L. Fuchs and C. Trädgårdh, "Large Eddy Simulations of mixing in

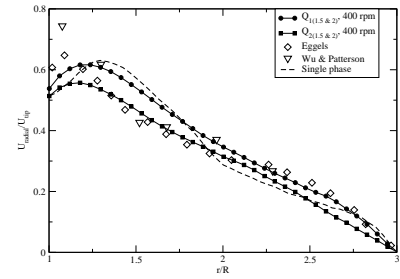


Fig. 3. Time averaged liquid velocity in (upper) radial, (middle) tangential and (lower) axial direction. The intersection is at $z=H/2$.

- an impinging jet", *Proc. of the 4th ECCOMAS Comp. Fluid Dynamics Conf.*, pp. 1169-1174, 1998.
- [6] P.C. Friberg and B.H. Hjertager, "Simulation of a 3-dimensional large-scale fermenter with four Rushton turbines using a two-fluid model", *Proc. of Third International Conference on Multi-phase Flows*, 1998.
- [7] J.-S. Wu, G.K. Patterson and M. van Doorn, "Distribution of turbulence energy dissipation rates in a Rushton turbine stirred mixer", *Experiments in Fluids*, vol. 8, pp. 153-160, 1989.
- [8] J.G.M. Eggels, "Direct and large-eddy simulation of turbulent fluid flow using the lattice-Boltzmann

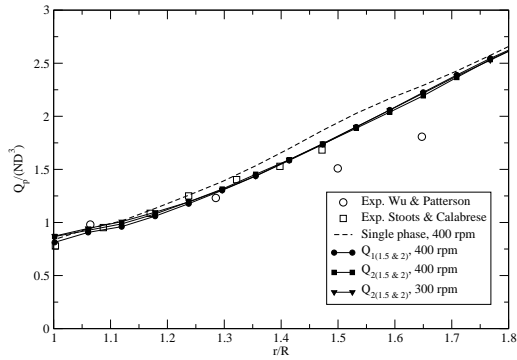


Fig. 4. Pumping capacity, compared to experimental data by Stoots and Calabrese [9] and Wu and Patterson [7]

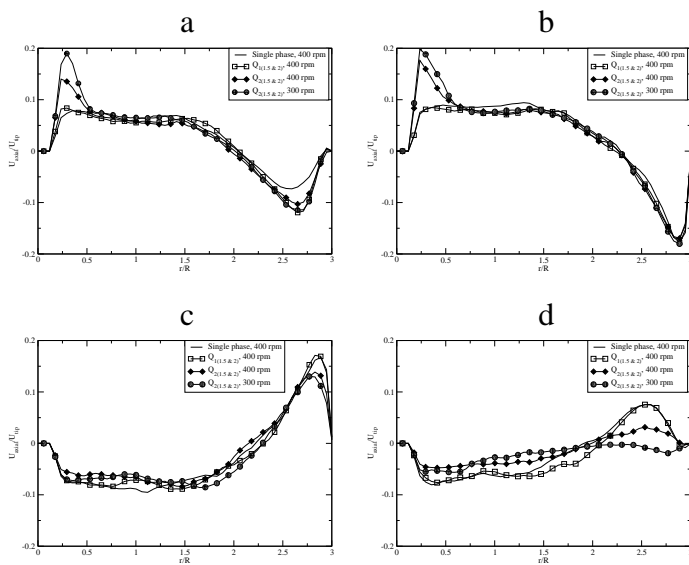


Fig. 5. Time averaged axial liquid velocity at (a) $z=2H/8$, (b) $z=3H/8$, (c) $z=5H/8$ and (d) $z=6H/8$.

scheme”, *Int. J. Heat and Fluid Flow*, vol. 17, pp. 307-323, 1996.

[9] C.M Stoots and R.V. Calabrese, ”Mean Velocity Field Relative to a Rushton Turbine Blade”, *AIChE J.*, vol. 41, pp. 1-11,1995.

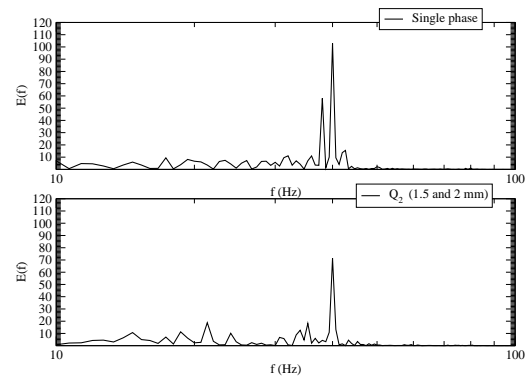


Fig. 6. Power spectrum at point location $r/R=1.5$, $\theta = 0$ and $z=H/2$ for single and Q_2 case.